Electronic Supplementary Information

Oxygen incorporated solution-processed high-κ La_2O_3 dielectrics with large-area uniformity, low leakage and high breakdown field comparable with ALD deposited films

Longsen Yan,‡[a] Waner He,‡[a] Xiaoci Liang,[b] Chuan Liu,*[b] Xihong Lu,[c] Chunlai Luo,[a] Aihua Zhang,[a] Ruiqiang Tao,[a] Zhen Fan,[a] Min Zeng,[a] Honglong Ning,[d] Guofu Zhou,[e] Xubing Lu,*[a] and Junming Liu[af]

[a] Institute for Advanced Materials, South China Academy of Advanced Optoelectronics, and Guangdong Provincial Key Laboratory of Optical Information Materials and Technology, South China Normal University
Guangzhou 510006, China
Email: luxubing@m.scnu.edu.cn (X. B. L.)

[b] State Key Laboratory of Optoelectronic Materials and Technologies, School of Electronics and Information Technology, Sun Yat-Sen University
Guangzhou 510274, China
Email: liuchuan5@mail.sysu.edu.cn (C. L.)

[c] MOE of the Key Laboratory of Bioinorganic and Synthetic Chemistry, The Key Lab of Low-carbon Chem and Energy Conservation of Guangdong Province, KLGHEI of Environment and Energy Chemistry, School of Chemistry, Sun Yat-Sen University
Guangzhou 510275, China

[d] State Key Laboratory of Luminescent Materials and Devices, Institute of Polymer Optoelectronic Materials and Devices, South China University of Technology
Guangzhou 510640, China

[e] Institute of Electronic Paper Displays and Guangdong Provincial Key Laboratory of Optical Information Materials and Technology, South China Academy of Advanced Optoelectronics, South China Normal University
Guangzhou, 510006, China

[f] Laboratory of Solid State Microstructures and Innovation Center of Advanced Microstructures, Nanjing University
Nanjing 210093, China

‡ These authors contributed equally: Longsen Yan, Waner He.

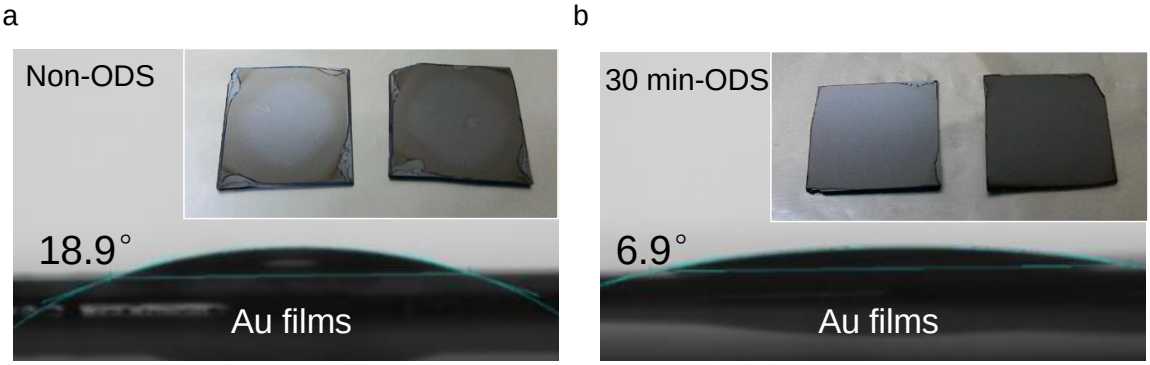

Figure S1 Contact angle images of the spin coating solution dipped on the Au film. a) non-O_2 solution; b) 30-min O_2 solution. The insets of Figure S1a and b show the surface images of the spin-coated La_2O_3 films. The film made from 30-min O_2 solution shows a much smaller contact angle than that from the non-O_2 solution. Consequently, the La_2O_3 film formed by 30-min O_2 solution shows a smoother and more uniform surface than that formed by non-O_2 solution.

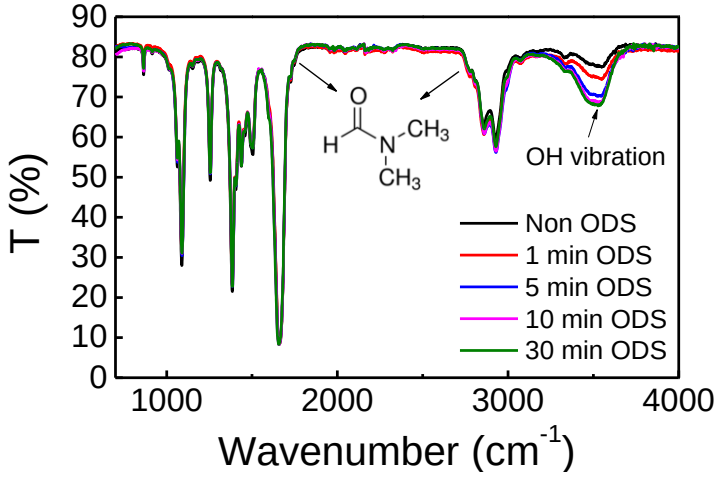

Figure S2 Fourier transform infrared spectroscopy measurement results of the solutions with different oxygen doping time. The solution with a longer O_2 infusion time has a a stronger OH vibration signal, demonstrating that oxygen infusion is efficient to produce OH bonding in the La_2O_3 solution.

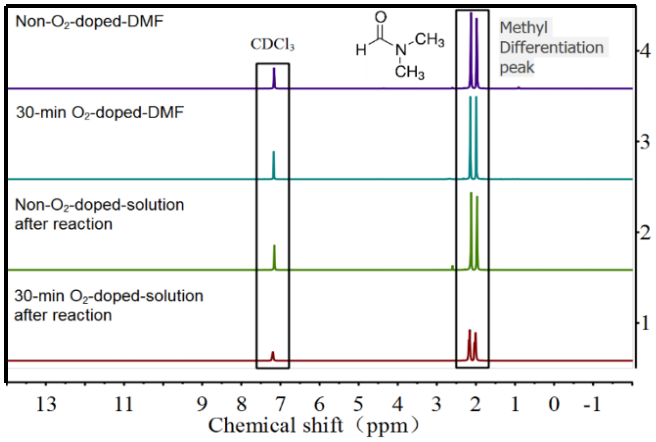

Figure S3 The ^{1}H-NMR characterization of precursor solutions.

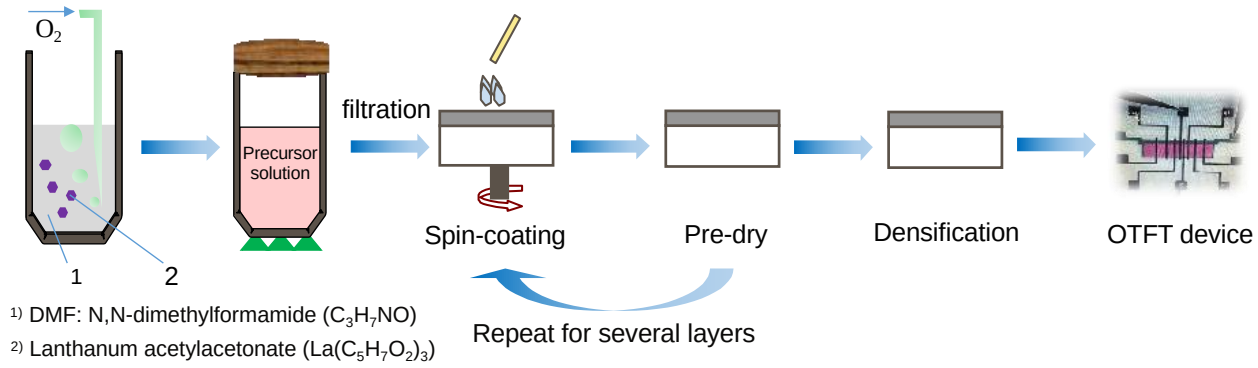

Figure S4 A schematic diagram of the deposition of the La_2O_3 thin films by using solution process.

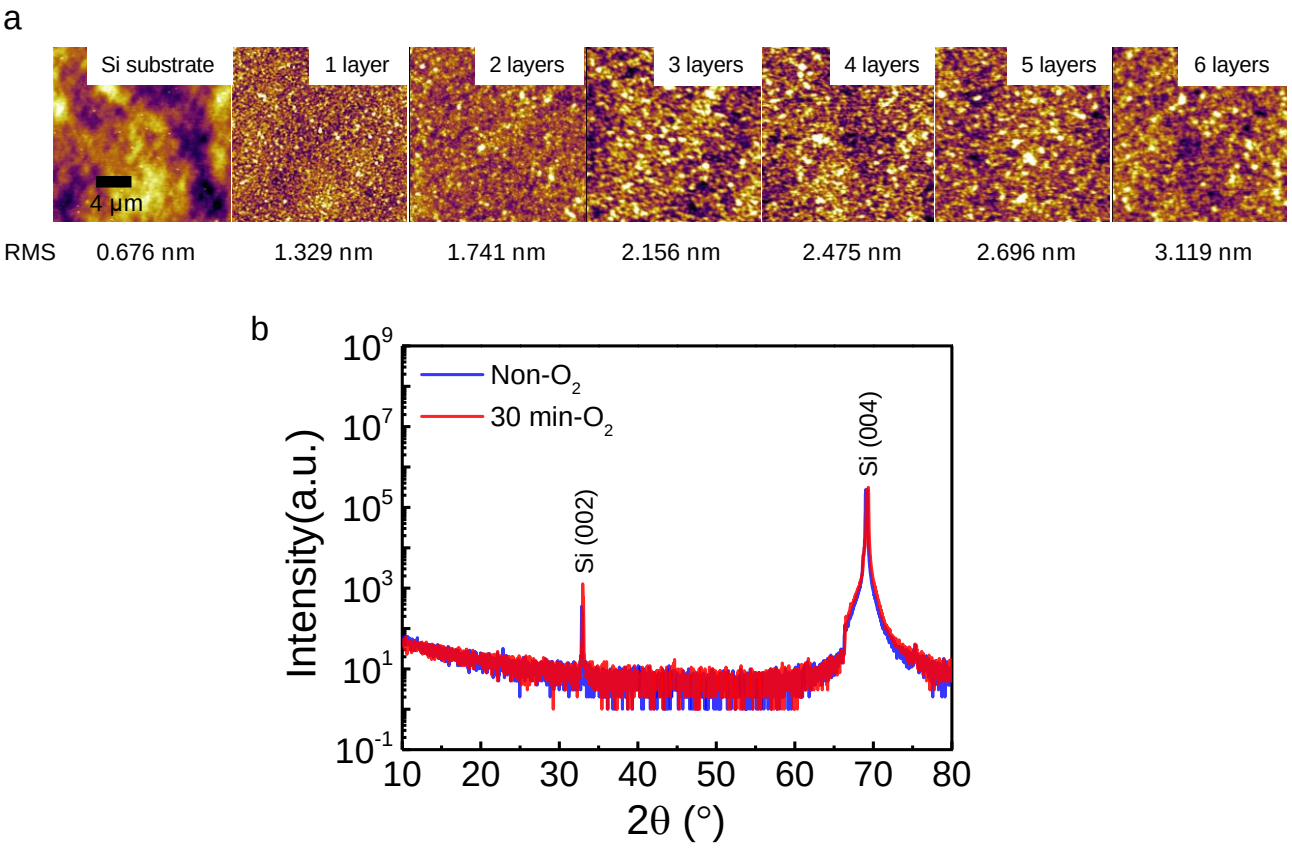

Figure S5 AFM images and XRD patterns. a) AFM images of La_2O_3 films and b) XRD patterns of the 120°C annealed La_2O_3 thin films by using non-O_2 and 30 min-O_2 solutions.

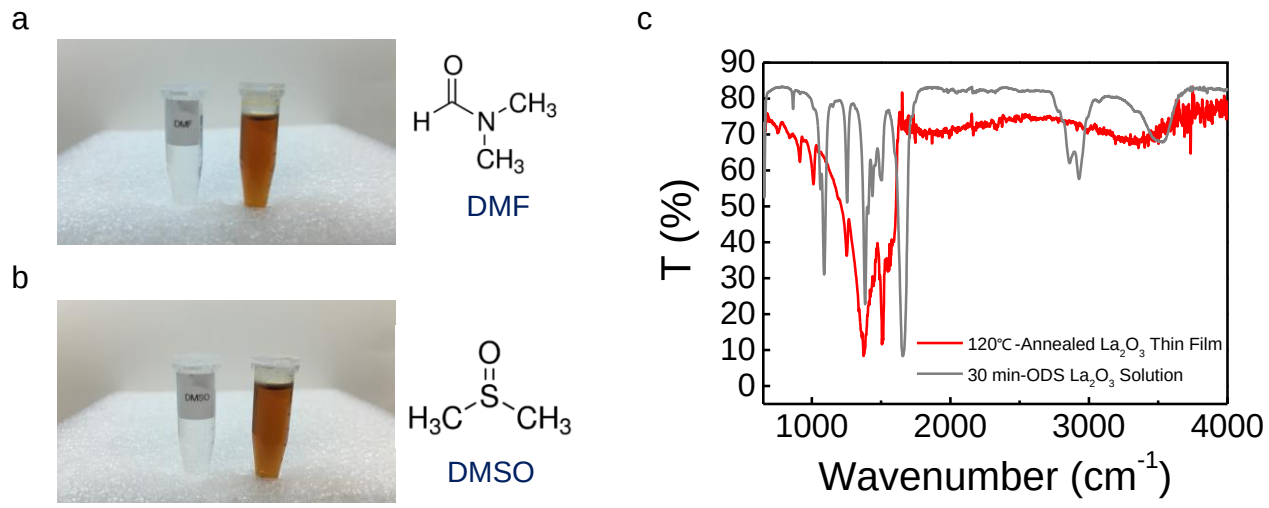

Figure S6 Optical micrographs of various 30-min-O_2 solutions after 12-hour reaction. a) DMF solvent and solution with $La(C_5H_7O2)_3 \cdot xH_2O$ dissolved in DMF. b) DMSO solvent and solution with $La(C_5H_7O_2)_3 \cdot xH_2O$ dissolved in DMSO. c) FT-IR measurement results of 30-min-O_2 solution and 120℃-annealed La_2O_3 thin film.

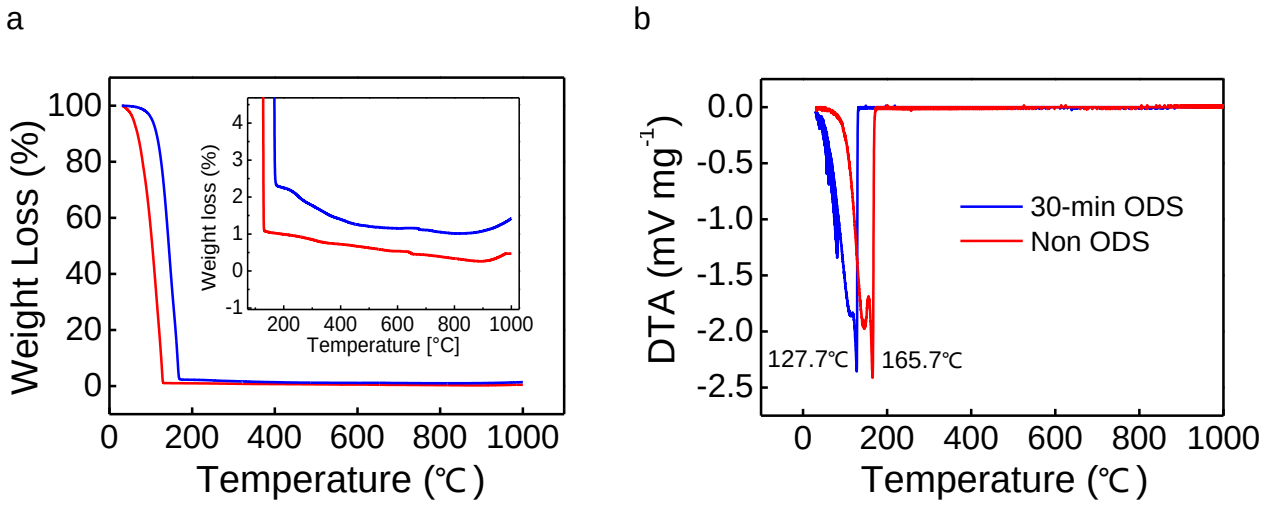

Figure S7 The thermal gravity and differential thermal analysis measurement results. a) The thermal gravity and b) differential thermal analysis measurement results of the non-O_2 and 30-min-O_2 solutions. The inset of Figure S7a shows a magnification of the curves at critical changes of weight loss.

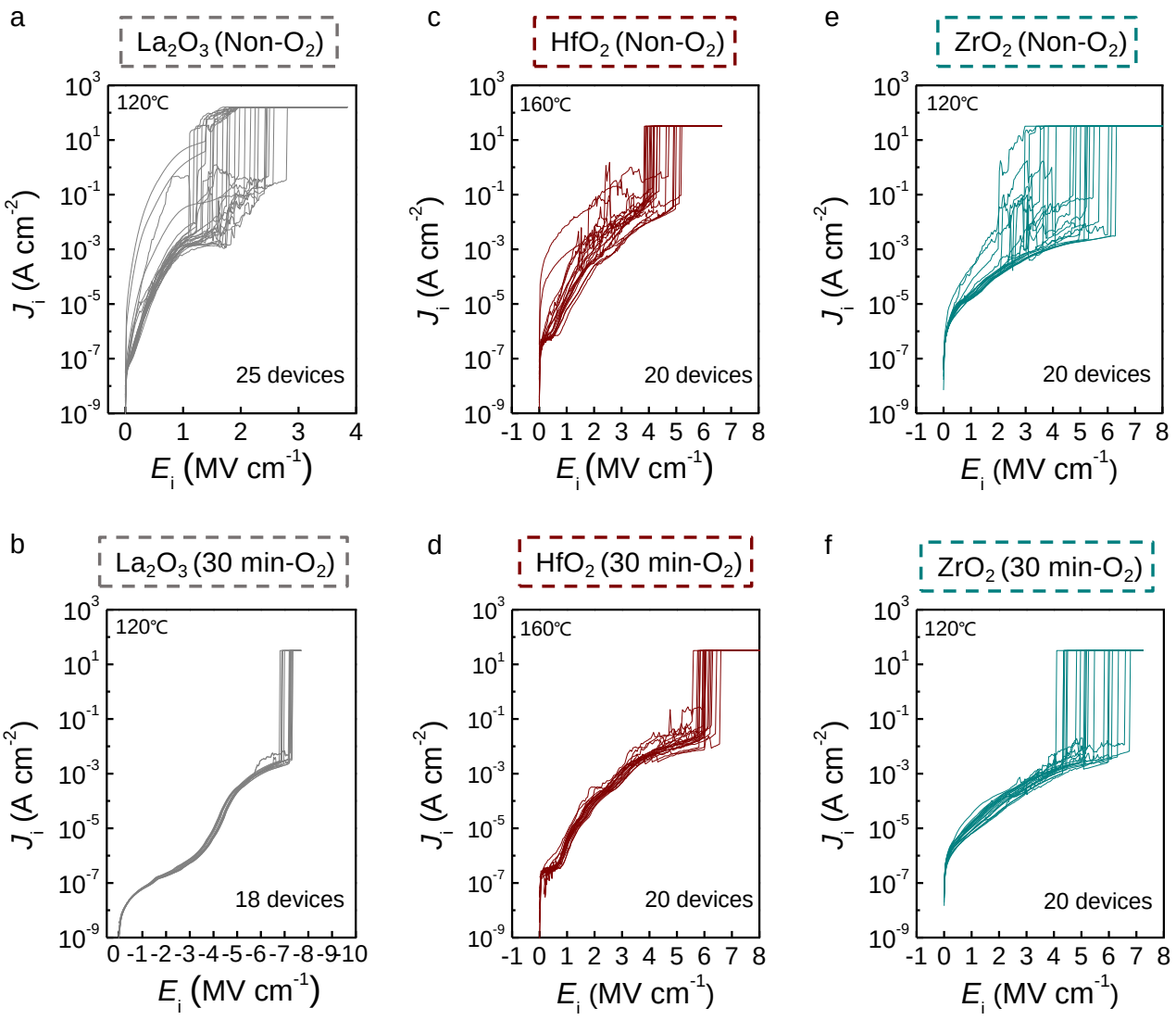

Figure S8 Leakage current as function of electric field characteristics of various dielectric films. a) La_2O_3 deposited by non-O_2 solution; b) La_2O_3 deposited by 30 min-O_2 solution; c) HfO_2 deposited by non-O_2 solution; d) HfO_2 deposited by 30 min-O_2 solution; e)ZrO_2 deposited by non-O_2 solution; f) ZrO_2 deposited by 30 min-O_2 solution. All of the films were deposited on the heavily doped Si substrate.

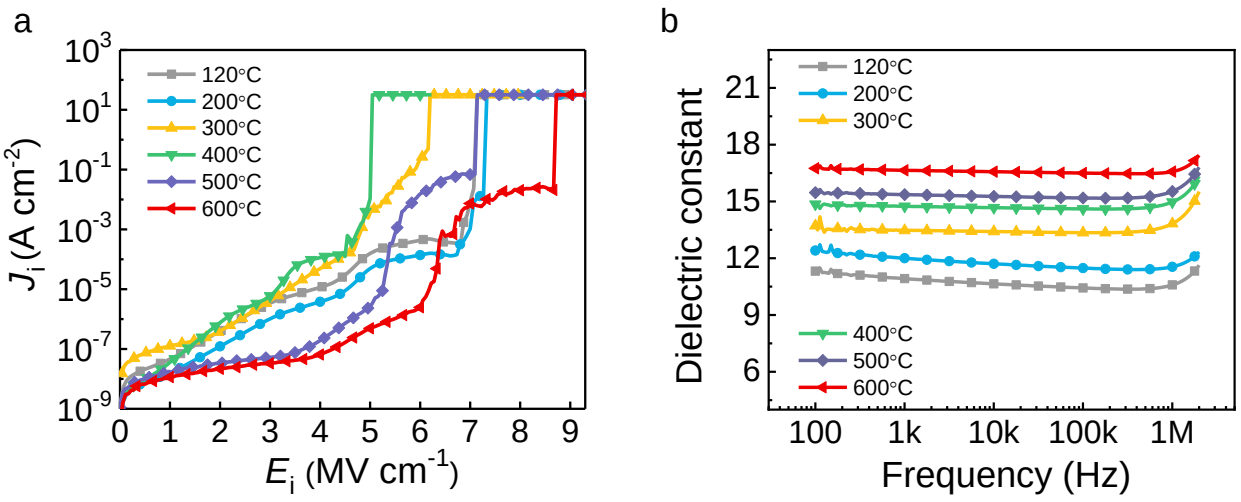

Figure S9 Insulating and dielectric properties for the 30-min-O_2 La_2O_3 films with different processing temperature (from 160°C to 600°C), manifested as a) the current density as a function of electric field (J_i-E_i curves) and b) permittivity as a function of testing frequency (from 100 to 2 MHz).

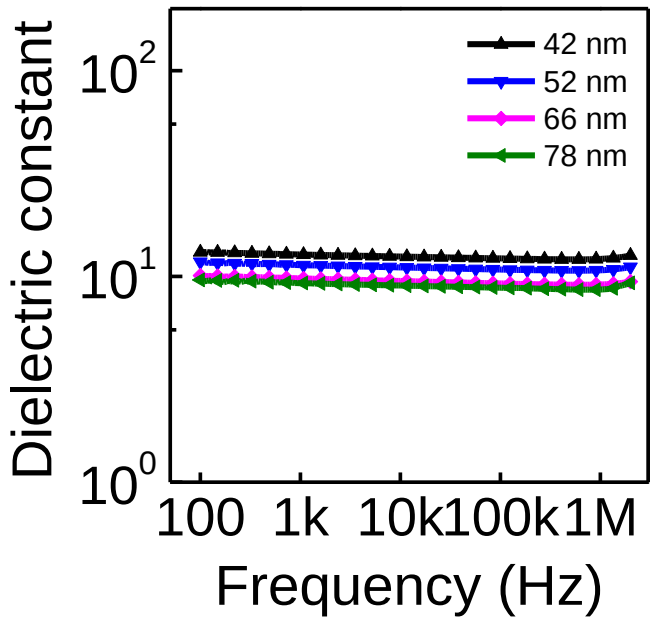

Figure S10 Dielectric properties of MIM devices with different spin-coated cycles (three to six cycles, approximately 42 nm to 78 nm): frequency dependent permittivity.

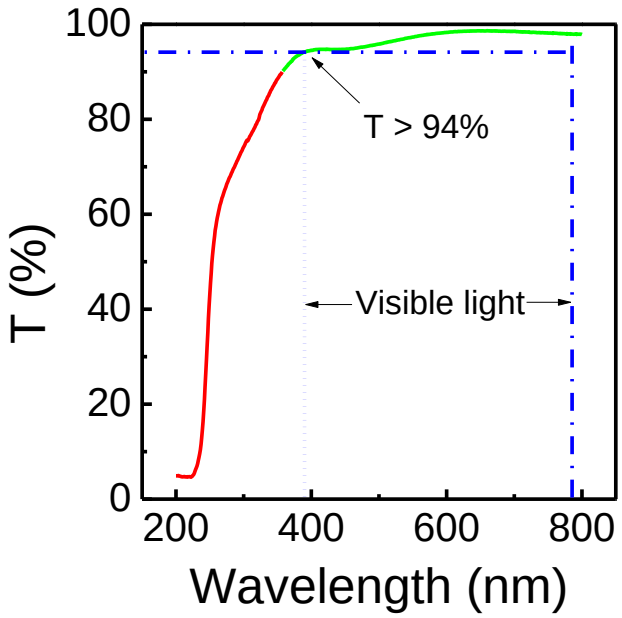

Figure S11 Optical transmittance spectrum of La_2O_3 thin film (26 nm) fabricated on 250 μm PET substrate. The measurement wavelength varies from 200 nm to 800 nm. Transmittance higher than 94 % is observed during the whole visible light range, indicating high potential application in the future transparent electronics.

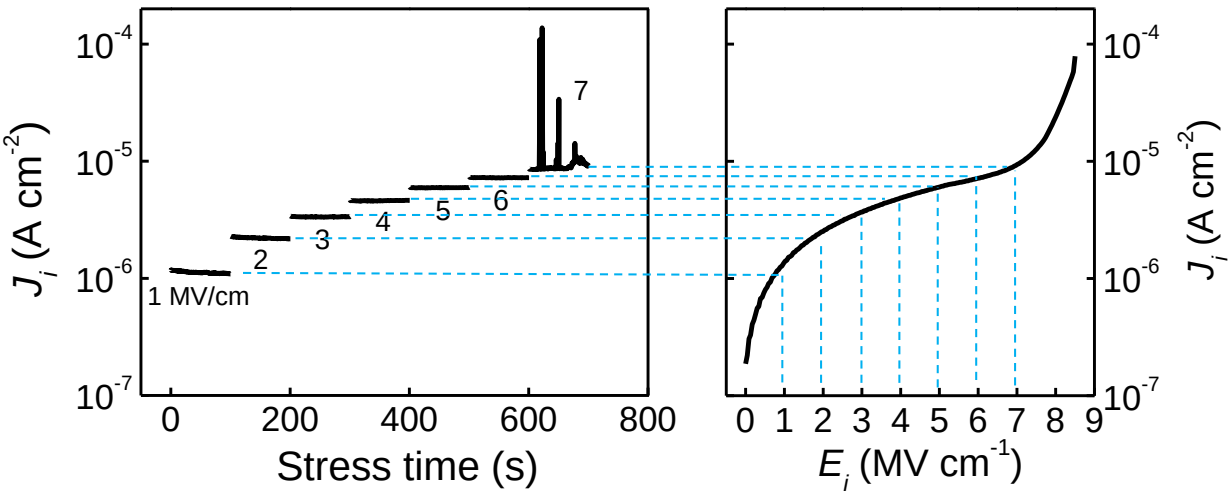

Figure S12 Electrical properties of ALD grown Al_2O_3 dielectric films. Leakage current as a function of stress time under various electric field and J_i-E_i characteristics showing the breakdown field.

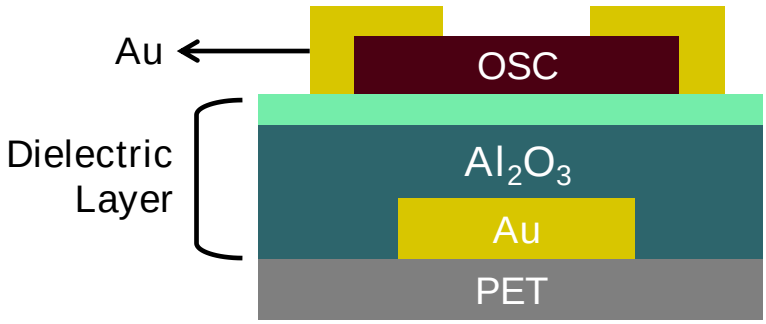

Figure S13 A schematic diagram of the cross-sectional structure of the La_2O_3-OTFT devices.

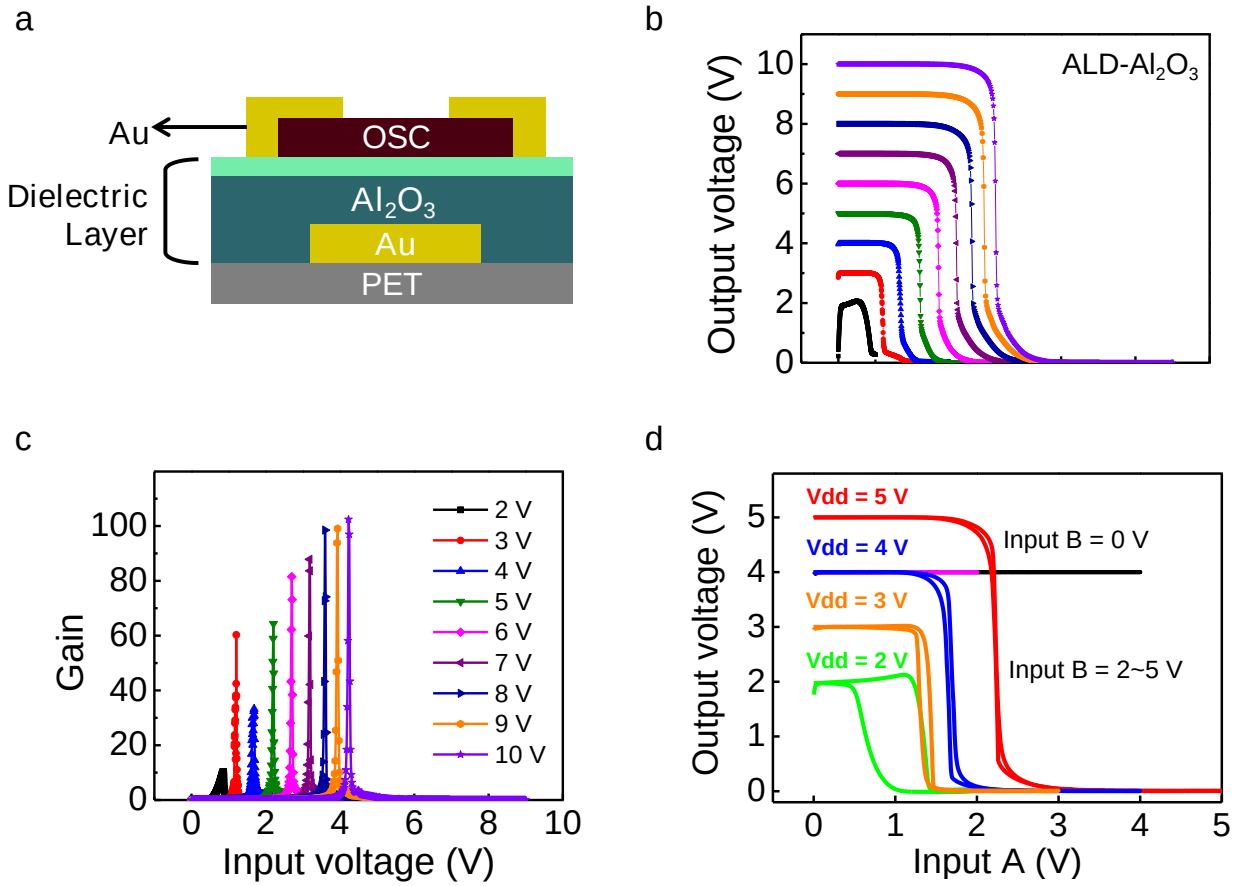

Figure S14 Electrical properties of complementary circuits with ALD grown Al_2O_3 dielectric films fabricated on flexible PET substrate. a) Schematic diagram of the cross-sectional structure of flexible ALD-Al_2O_3 OTFTs. b) Output and c) small-signal gain as a function of input voltage for supply voltages between 2 and 10 V. d) Transfer characteristics of two-input NAND gate using ALD-Al_2O_3 as a gate dielectric.

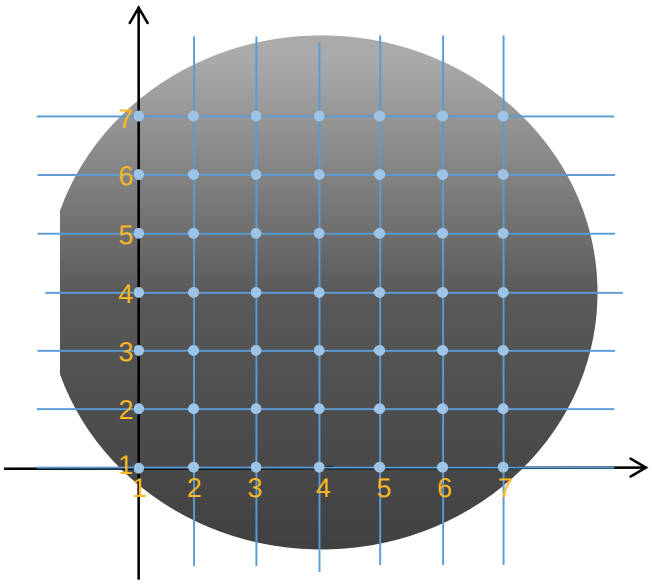

Figure S15 A schematic diagram of the location for thickness measurement spots on 2-inch wafer-scale La_2O_3 film.

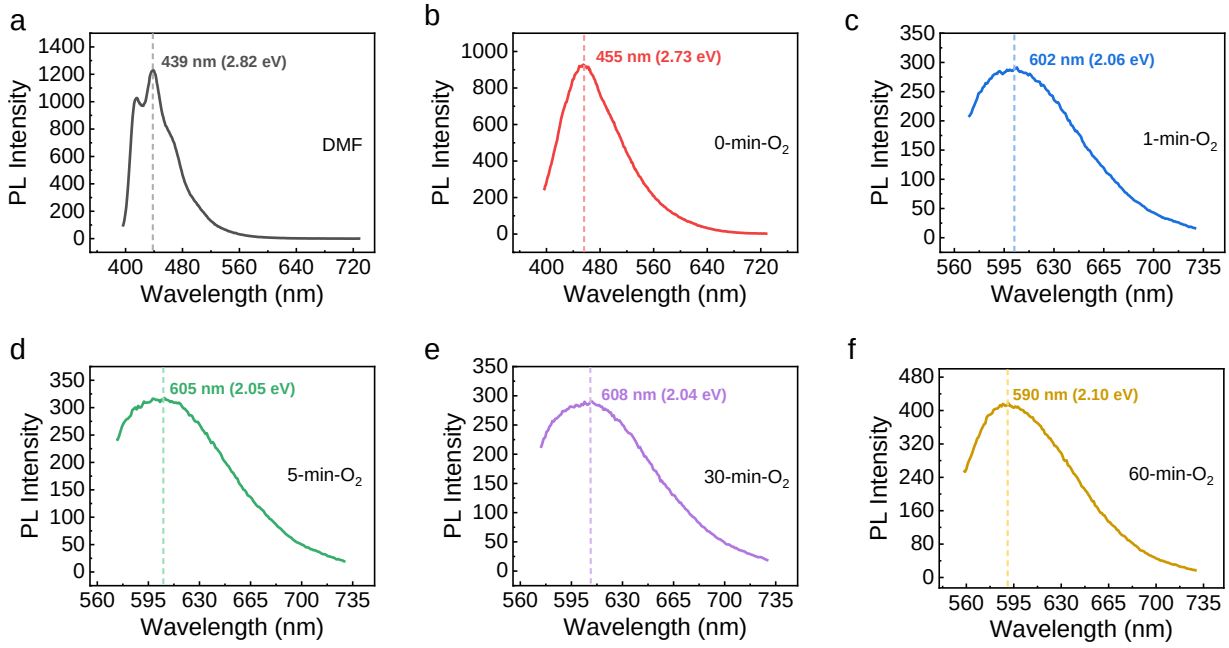

Figure S16 Photoluminescence (PL) emission spectra of a) DMF solvent and b-f) precursor solution with various oxygen infusion times (from 0 minute to 60 minute) after 12-hour reaction.

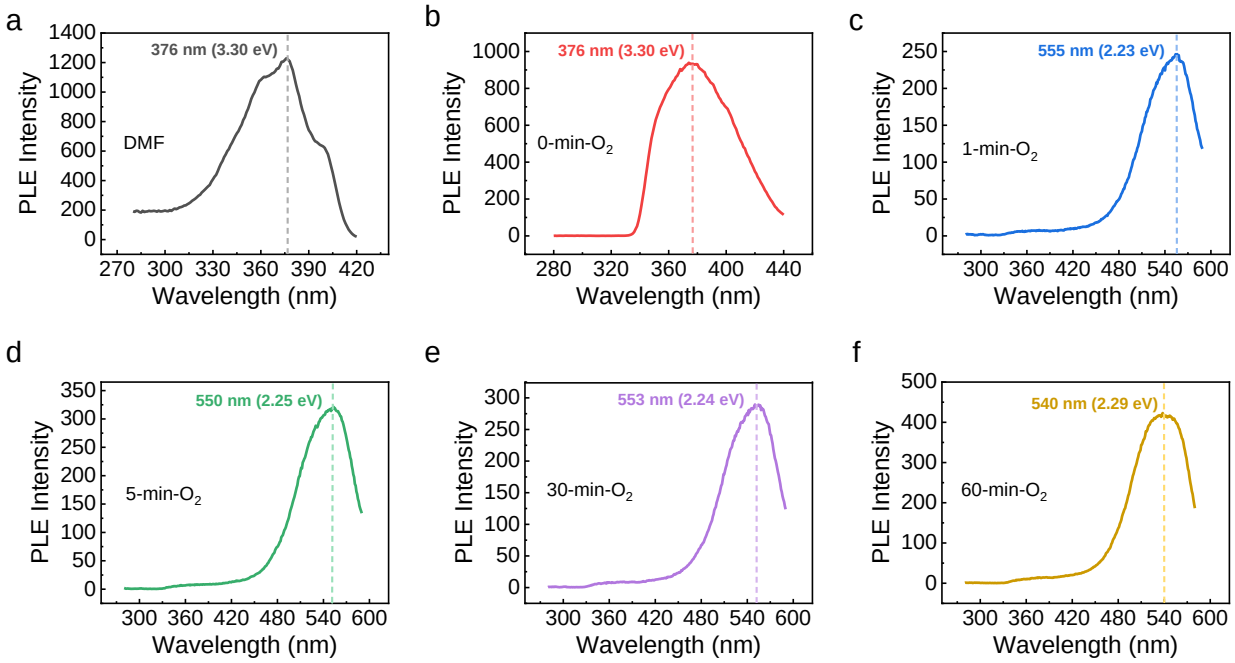

Figure S17 Photoluminescence excitation (PLE) spectra of a) DMF solvent and b-f) precursor solution with various oxygen infusion times (from 0 minute to 60 minute) after 12-hour reaction.

Table S1 Data from literatures for Fig. 2b in the main context.

Dielectric	Coating method [a]	Process temp.(℃)	κ	Band gap(eV)	Leakage (A cm^{-2}) @1MV	Leakage (A cm^{-2}) @2.5MV	E_b (MV cm^{-1})	Semiconductor	μ	V_{Th} (V)	on/off ratio	Year
[1]AlOx	SP	400	~9.2	5.62	--	--	~1.8	ZnO	7		~10^5	2011
[2]AlOx	SC	300	~6.3	--	10^{-5}	~	~4	ZTO	33	1.2	~10^8	2011
[3]AlOx	SC	350	--	--	--	--	~4	ZnO:Li	46.9	0.2	~10^5	2013
[4]AlOx	SC	300	10.1	--	--	--	>2	InO	21.7		~10^4	2014
[5]AlOx	SC	350	--	--	10^{-5}	10^{-4}	4.9	IGZO	84.4	1.0	~10^5	2014
[6]AlOx	SC	300	11.4	--	10^{-7}	10^{-5}	--	IZO	10.1	2.07	~10^5	2015
[7]AlOx	SCS	350	7.07	5.6	--	--	8.2	IGZO	19.8	3	~10^5	2016
[8]ZrOx	SC	250	12.1	--	10^{-7}	10^{-5}	~3.94	InO	39.3		~10^7	2013
[9]ZrOx	SC	350	14.8	5.4	10^{-8}	10^{-7}	~2.8	IZO	7.21		~10^6	2013
[10]ZrOx	SC	300	12.5	--	10^{-9}	10^{-8}	7.2	InO	23		~10^7	2014
[11]ZrOx	SC	300	22.6	3.0	10^{-6}	~	>2	InO	1.6		~10^4	2014
[12]ZrOx	SC	450	16.1	--	10^{-6}	10^{-5}	3.2	ITZO/IGZO	40	3	~10^6	2014
[13]ZrOx	IJ	500	22	--	10^{-6}	10^{-4}	4	SnO	11	<5	~10^6	2015
[14]ZrOx	SC	250	13	--	10^{-6}	10^{-4}	>5	IZO	75	0.22	~10^4	2015
[15]ZrOx	SC	350	--	--	--	--	--	IZO	93.4		~10^5	2015
[16]ZrOx	SCS	350	14.3	5.6	10^{-7}	~	9.5	IGZO	28.5	3	~10^5	2016
[17]HfOx	SC	400	~13	--	10^{-3}	10^{-2}	~5.5	IGZO	13.1	8.5	~10^7	2011
[18]HfOx	SC	300	~14	3.5	--	--	--	ZTO	1.05	1.18	~10^5	2012
[19]HfOx	SC	450	18.5	5.7	10^{-6}	10^{-4}	>2.5	ZnO	42	2	~10^5	2015
LaOx	**SC**	**120**	**12.9**	**6.3**	**10^{-8}**	**10^{-7}**	**>7**	**Pentacene**	**0.37**	**-0.59**	**~10^5**	

[a] Abbreviation for coating method: SC: Spin-coating; SP: spray pyrolysis; IJ: Inkjet; SCS: Spray-combustion synthesis;

[b] -- : Not reported or not mentioned.

References

1 G. Adamopoulos, S. Thomas, D. D. C. Bradley, M. A. McLachlan and T. D. Anthopoulos, *Appl. Phys. Lett.* 2011, **98**, 123503.

2 C. Avis and J. Jang, *J. Mater. Chem.* 2011, **21**, 10649-10652.

3 J. H. Park, K. Kim, Y. B. Yoo, S. Y. Park, K.-H. Lim, K. H. Lee, H. K. Baik and Y. S. Kim, *J. Mater. Chem. C* 2013, **1**, 7166.

4 W. Xu, H. Wang, L. Ye and J. Xu, *J. Mater. Chem. C* 2014, **2**, 5389-5396.

5 Y. S. Rim, H. Chen, Y. Liu, S.-H. Bae, H. J. Kim, and Y. Yang, *ACS Nano* 2014, **8**, 9680-9698.

6 W. Xu, H. Wang, F. Xie, J. Chen, H. Cao and J. B. Xu, *ACS Appl. Mater. Interfaces* 2015, **7**, 5803-5810.

7 B. Wang, X. Yu, P. Guo, W. Huang, L. Zeng, N. Zhou, L. Chi, M. J. Bedzyk, R. P. H. Chang, T. J. Marks and A. Facchetti, *Adv. Electron. Mater.* 2016, **2**, 1500427.

8 J. H. Park, Y. B. Yoo, K. H. Lee, W. S. Jang, J. Y. Oh, S. S. Chae, H. W. Lee, S. W. Han and H. K. Baik, *ACS Appl. Mater. Interfaces* 2013, **5**, 8067-8075.

9 J. H. Park, Y. B. Yoo, K. H. Lee, W. S. Jang, J. Y. Oh, S. S. Chae and H. K. Baik, *ACS Appl. Mater. Interfaces* 2013, **5**, 410-417.

10 A. Liu, G. X. Liu, H. H. Zhu, F. Xu, E. Fortunato, R. Martins and F. K. Shan, *ACS Appl. Mater. Interfaces* 2014, **6**, 17364-17369.

11 W. Xu, H. Wang, L. Ye and J. Xu, *J. Mater. Chem. C* 2014, **2**, 5389-5396.

12 Y. S. Rim, H. Chen, X. Kou, H. S. Duan, H. Zhou, M. Cai, H. J. Kim and Y. Yang, *Adv. Mater.* 2014, **26**, 4273-5278.

13 J. Jang, H. Kang, H. C. N. Chakravarthula and V. Subramanian, *Adv. Electron. Mater.* 2015, **1**, 1500086.

14 M. Hasan, M.-C. Nguyen, H. Kim, S.-W. You, Y.-S. Jeon, D.-T. Tong, D.-H. Lee, J. K. Jeong and R. Choi, *Thin Solid Films* 2015, **589**, 90-94.

15 X. Yu, J. Smith, N. Zhou, L. Zeng, P. Guo, Y. Xia, A. Alvarez, S. Aghion, H. Lin, J. Yu, R. P. Chang, M. J. Bedzyk, R. Ferragut, T. J. Marks and A. Facchetti, *Proc. Natl. Acad. Sci. U. S. A*. 2015, **112**, 3217-3222.

16 B. Wang, X. Yu, P. Guo, W. Huang, L. Zeng, N. Zhou, L. Chi, M. J. Bedzyk, R. P. H. Chang, T. J. Marks and A. Facchetti, *Adv. Electron. Mater.* 2016, **2**, 1500427.

17 K. Jiang, J. T. Anderson, K. Hoshino, D. Li, J. F. Wager and D. A. Keszler, *Chem. Mater.* 2011, **23**, 945-952.

18 C. Avis, Y. G. Kim and J. Jang, *J. Mater. Chem.* 2012, **22**, 17415-17420.

19 M. Esro, G. Vourlias, C. Somerton, W. I. Milne and G. Adamopoulos, *Adv. Funct. Mater.* 2015, **25**, 134-141.